New ^{146}Nd(n,γ) measurement at CERN n_TOF

Activation campaign at n_TOF NEAR

B. Gameiro, J. Lerendegui-Marco, C. Domingo-Pardo, G. Auñón, V. Babiano-Suárez, M. Bacak, J. Balibrea-Correa, J. Bartolomé, F. Calviño, A. Casanovas, G. Cortés, S. Cristallo, B. Fernández, G. de la Fuente, C. Guerrero, S. Kopanos, U. Köster, I. Ladarescu, C. Lederer, M. Lugaro, N. Liuç, E. Odusina, P. Péres, A. Reina, G. Rovira, B. Soós, N. Sosnin, B. Szányi, A. Tarifeño-Saldivia, P. Torres-Sánchez, D. Vescovi and the n_TOF Collaboration

XL Reunión Bienal de la RSEF
20-24 July 2026, Sevilla

2026/07/20

1. Motivation & Project Summary
2. Activation experiment at n_TOF-NEAR
3. Progress and results
4. Conclusion

Motivation: s process & SiC grains

- S-process around ^{146}Nd
- Relevant in the Asymptotic Giant Branch (AGB) phase of stars

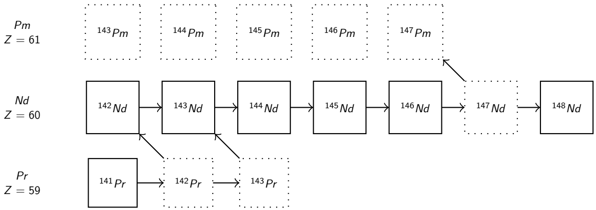

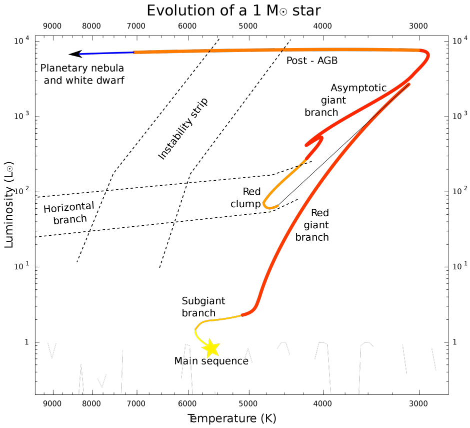

Motivation: Astrophysics

Geochimica et Cosmochimica Acta
Volume 221, 15 January 2018, Pages 200-218

Rare earth element abundances in presolar SiC

T.R. Ireland [a b], J.N. Ávila [a b], M. Lugaro [c], S. Cristallo [d], P. Holden [a], P. Lanc [a], L. Nittler [e], C.M.O'D. Alexander [e], F. Gyngard [f], S. Amari [f]

https://doi.org/10.1016/j.gca.2017.05.027 Get rights and content

4. Discussion

4.2. Interpreting trace-element abundances in presolar SiC

4.2.3. Neodymium

The Nd anomalies apparent in Fig. 10 (envelope compositions normalised to solar) and Fig. 11 (SiC compositions normalised to *s*-process predictions) are therefore related to the model predictions for the abundance of ^{146}Nd. We note that Yin et al. (2006) plotted Nd isotope compositions and showed that the Arlandini et al. (1999) ^{146}Nd/^{144}Nd ratio is elevated by ~15% compared to meteoritic SiC. Of relevance here, in the theoretical predictions from Arlandini et al. (1999) and those computed with the FUNS code (Cristallo et al., 2009, Cristallo et al., 2011, Cristallo et al., 2015) for which the neutron-capture cross section for ^{146}Nd is taken from Bao et al. (2000). A somewhat higher neutron-capture cross section would lead to a better agreement between the SiC data and the stellar predictions. We therefore conclude that the ^{146}Nd *s*-process deviation as presented may be an artefact caused by an overproduction of ^{146}Nd by stellar models and as such stellar theoretical predictions of this nuclide must be re-evaluated.

THE ASTROPHYSICAL JOURNAL

Signatures of the *s*-Process in Presolar Silicon Carbide Grains: Barium through Hafnium

Qing-Zhu Yin[1], Cin-Ty Aeolus Lee[2], and Ulrich Ott[3,4]

The Astrophysical Journal, Volume 647, Number 1
Citation Qing-Zhu Yin *et al* 2006 *ApJ* **647** 676
DOI 10.1086/505188

3. RESULTS AND DISCUSSION

3.1. Isotopic Compositions

Neodymium.— Some discrepancy, however, seems to exist at mass ^{146}Nd, where experimental data, both from TIMS and from our work (even more so after a ~10% correction to ^{145}Nd) indicate ^{146}Nd/^{144}Nd to be ~15% lower than theoretical expectations.

- Discrepancies between SiC data and model predictions
- Indication of higher cross-section

Motivation: Astrophysics

- Sensitivity calculations by D. Vescovi, S. Cristallo
- Data points refer to SiC presolar grains from $2M_{\odot}$
- REF: Bao & Kappeler 2000
- ASTRAL: re-evaluation by Reifarth 2018
- Largest deviation in $^{146}Nd/^{144}Nd$
- $^{146}Nd/^{144}Nd$ is very sensitive to $^{146}Nd(n,\gamma)$
- The kT=8keV is the most relevant stellar temperature
  - +15% change of the cross section below 20keV would solve the discrepancy

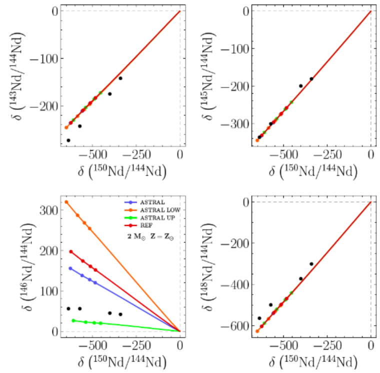

Motivation: Nuclear Data

- RRR based on transmission measurement
  - Filters, (n,total)
- Discrepancies between measurements for URR
  - The evaluation follows lowest uncertainty data, despite discrepancies

EXFOR: transmission measurement of Nd146

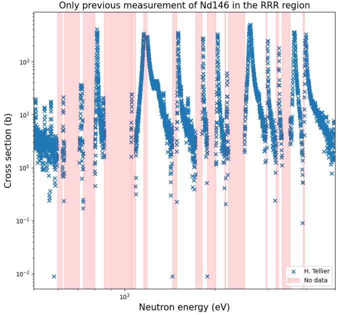

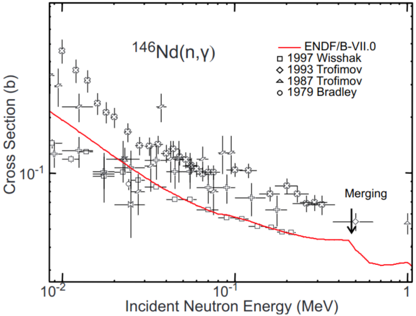

Plan: the full project of $^{146}Nd(n,\gamma)$

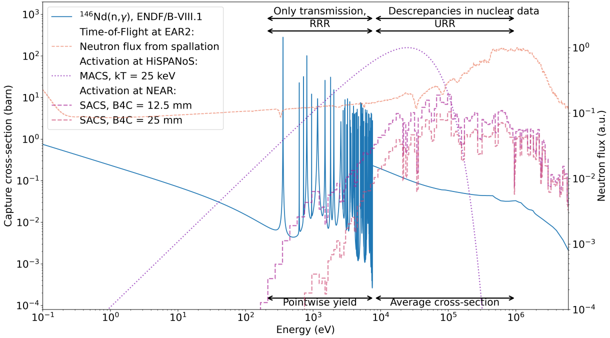

Figure 1: Overview of the $^{146}Nd(n,\gamma)$ project and its campaigns.

- TOF@n_TOF-EAR2: provides pointwise data (analysis ongoing)
- Activation@HiSPANoS-CNA: MACS from established facility (analysis ongoing)
- Activation@n_TOF-NEAR: SACS from new facility (analysis ongoing)
- The n_TOF-EAR2 and HiSPANoS-CNA campaigns contribute to the validation of the new NEAR facility.
- Today I'll focus on the multiple activations at NEAR, the new facility of n_TOF, where the ^{146}Nd campaign was the first approved activation proposal

NEAR: a new station at n_TOF

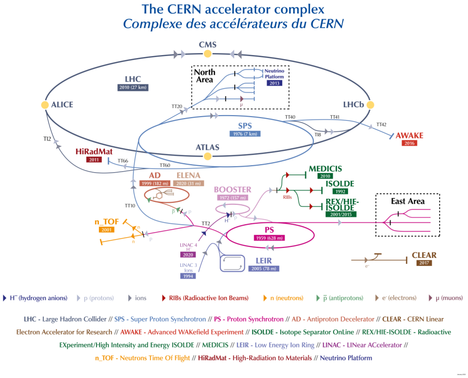

Figure 2: The CERN accelerator complex.

- n_TOF: CERN's neutron time-of-flight facility
  - Protons hit a heavy spallation target → pulsed, white neutron beam
  - Sent along flight paths to EAR1 and EAR2, the facility's two established TOF stations

NEAR: a new station at n_TOF

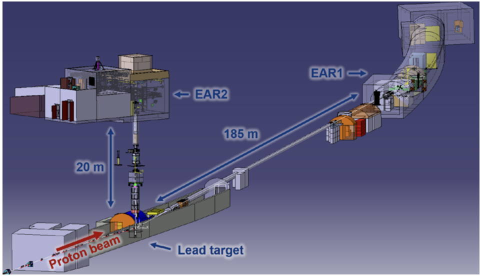

Figure 2: The n_TOF facility: spallation target, EAR1 and EAR2.

- n_TOF: CERN's neutron time-of-flight facility
- NEAR: a new station, right next to the spallation target
  - Very high flux, thanks to the short distance
  - Very short flight path → activation, not TOF, campaigns

NEAR: a new station at n_TOF

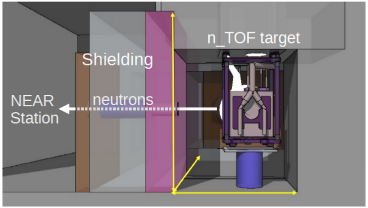

Figure 2: NEAR, next to the n_TOF spallation target and shielding.

Patronis et al., EPJ A 61, 128 (2025)

- n_TOF: CERN's neutron time-of-flight facility
- NEAR: a new station, right next to the spallation target
- Technique:
  - Irradiate sample with neutrons
  - Measure decay γ-rays in dedicated station

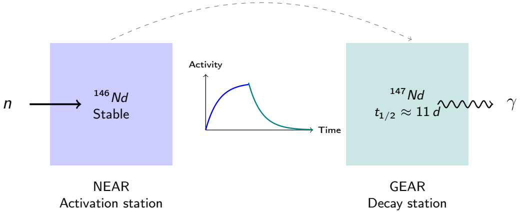

Activation station: setup & technique

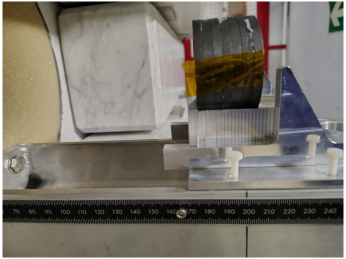

Figure 3: The activation station of NEAR.

- NEAR is the new activation facility of n_TOF
  - Has undergone several upgrades recently
  - 1st project with multiple facility crosscheck
  - 1st project of astrophysical interest
- Technique: ^{146}Nd stable, ^{147}Nd radioactive, $T_{1/2} \approx 11$d → suitable for activation

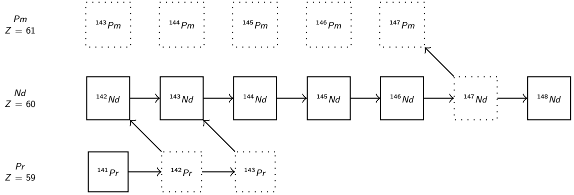

Activation station: setup & technique

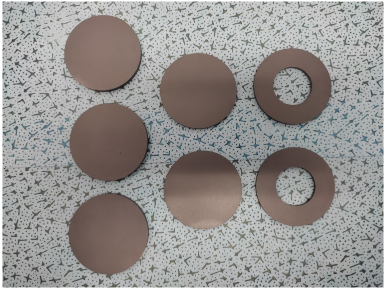

Figure 3: B_4C moderators of different thicknesses to shape the neutron flux.

- NEAR is the new activation facility of n_TOF
- Technique: ^{146}Nd stable, ^{147}Nd radioactive, $T_{1/2} \approx 11$d $\rightarrow$ suitable for activation
- Filter system
  - Based on B_4C, filters neutrons at low energy
  - Different front thicknesses give different fluxes (effectively thresholds)
  - Side/back filters reduce scattered-neutron contribution
- New moderator: Al_2O_3, filters neutrons at high energy
- Direct output: SACS of ^{147}Nd and of Au; final aim: MACS of ^{146}Nd relative to MACS of Au
  - NEAR's flux is not Maxwellian $\rightarrow$ requires simulating the flux shape inside the B_4C filters

Decay station: setup & technique

Figure 4: The decay station of GEAR.

- The HPGe with shielding of GEAR was used
  - Shielding & Resolution: low background, high resolution → selects specific γ-rays even in complex spectra
  - Fixed measuring positions: reproducibility, well-characterized efficiency curves; balances efficiency, measurement time, and position uncertainty

Decay station: setup & technique

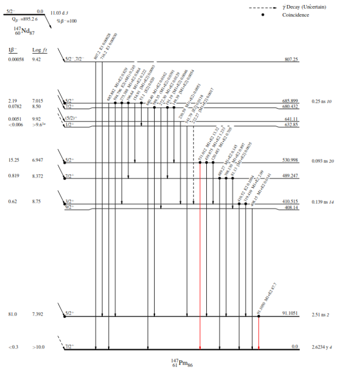

Figure 4: Decay scheme of ^{147}Nd.

- The HPGe with shielding of GEAR was used
- Two decay lines of interest: 91 keV (I≈29%), 531 keV (I≈13%)
  - Focus on 531 keV: better established efficiency calibration

Decay station: setup & technique

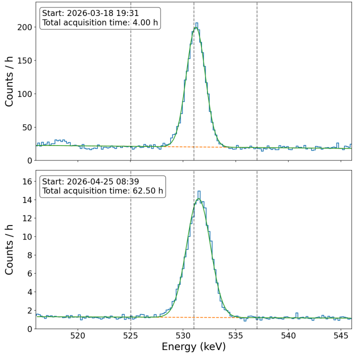

Figure 4: 531 keV photopeak: EOI (top) and end-of-measurement (bottom).

- The HPGe with shielding of GEAR was used
- Two decay lines of interest: 91 keV (I≈29%), 531 keV (I≈13%)
  - Focus on 531 keV: better established efficiency calibration
- NEAR is only now starting experimental activity → improved MC modelling of the HPGe efficiency is required

Samples

Figure 5: Nd and other sample discs used in the n_TOF campaigns.

- Enriched ^{146}Nd oxide, 8 mm, 212.4 mg, 97.4% enr. $\rightarrow$ used for the filtered activations
- Natural Nd oxide, 8 mm, 373.5 mg $\rightarrow$ used for the unfiltered activation
- Au monitor foil, 8 mm, co-irradiated with each sample for flux normalization

Progress and results: three analysis fronts

- **^{147}Nd half life**
  - First results: new half-life measurement
- **HPGe detector efficiency**
  - Characterization and MC optimization
  - Development of a Bayesian-optimisation methodology for detector characterization
- **Neutron flux shape 3**
  - Simulation of NEAR experimental area
  - NEAR beam and B_4C filter simulations
  - Essential for MACS/SACS extraction

Half life of ^{147}Nd

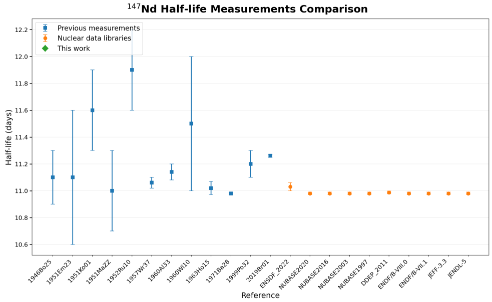

Figure 6: Comparison of the half life of ^{147}Nd from previous measurements and nuclear data libraries.

- Most of the previous measurements are based on the total number of decays from a very pure sample of ^{147}Nd
- Most libraries use the value from 1971Ba28
- Only ENSDF2022 takes the measurement of 2019Br01 into account, which was based on the selection of γ-ray peaks from the decay of ^{147}Nd

Half life of ^{147}Nd

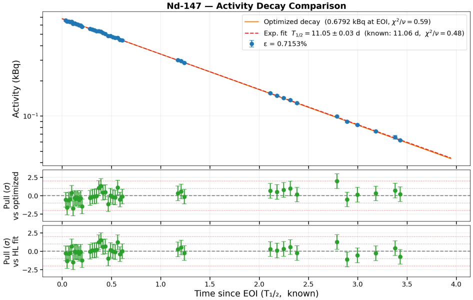

Figure 6: Decay of ^{147}Nd from the second activation campaign. The half life is extracted from a linear fit to the log of the data.

- Most of the previous measurements are based on the total number of decays from a very pure sample of ^{147}Nd
- Most libraries use the value from 1971Ba28
- Only ENSDF2022 takes the measurement of 2019Br01 into account, which was based on the selection of γ-ray peaks from the decay of ^{147}Nd
- The decay for the second activation was measured at a single distance of 9cm to avoid the efficiency issues and minimize the effects of alignment: (11.05±0.03)d

Half life of ^{147}Nd

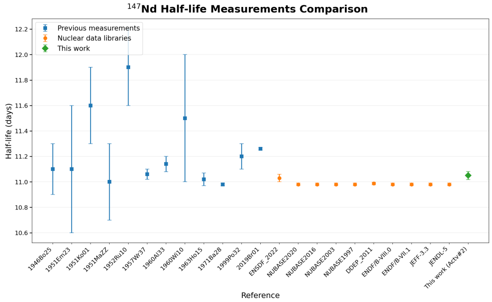

Figure 6: Comparison of the half life of ^{147}Nd from previous measurements, nuclear data libraries, and results from this campaign.

- Most of the previous measurements are based on the total number of decays from a very pure sample of ^{147}Nd
- Most libraries use the value from 1971Ba28
- Only ENSDF2022 takes the measurement of 2019Br01 into account, which was based on the selection of γ-ray peaks from the decay of ^{147}Nd
- The decay for the second activation was measured at a single distance of 9cm to avoid the efficiency issues and minimize the effects of alignment: (11.05 ± 0.03)d
- Valuable extra result beyond MACS/SACS: resolves prior half-life discrepancies
- Enabled by NEAR's high flux and the long GEAR measuring time

HPGe simulation: calibrating the detector response

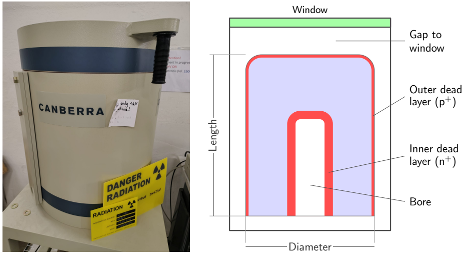

Figure 7: HPGe detector with Canberra electronics (left) and scheme of the detector with its main parameters (right).

- Efficiency depends on the detector's *effective* geometry (dead layer, crystal dimensions, air gap). Murphy et al. 2019: datasheet values can differ from the true response by up to 30%

HPGe simulation: calibrating the detector response

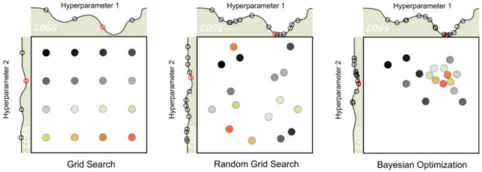

Figure 7: Grid search, random search, and Bayesian optimisation of a parameter space.

- Efficiency depends on the detector's *effective* geometry (dead layer, crystal dimensions, air gap). Murphy et al. 2019: datasheet values can differ from the true response by up to 30%
- **Problem**: brute-force grid search requires 7161 geometries (31 radii $\times$ 7 lengths $\times$ 33 gaps) — impractical to scale

HPGe simulation: calibrating the detector response

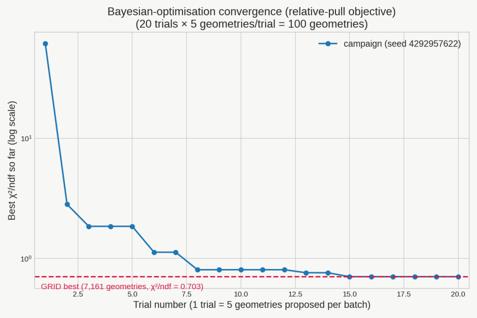

Figure 7: Best-so-far χ^2/ndf vs. trial for a Bayesian-optimisation campaign (100 geometries, relative-pull objective), against the grid search's best result.

- Efficiency depends on the detector's *effective* geometry (dead layer, crystal dimensions, air gap). Murphy et al. 2019: datasheet values can differ from the true response by up to 30%
- **Problem**: brute-force grid search requires 7161 geometries (31 radii $\times$ 7 lengths $\times$ 33 gaps) — impractical to scale
- **Solution**: Bayesian optimisation (fitted to ^{152}Eu efficiency data via a parametric Geant4 model, A. Reina) reduces this to $\sim$100 geometries per distance ($\sim$72$\times$ fewer simulations)
- The campaign converges to within 0.4% of the grid search's best result

HPGe simulation: calibrating the detector response

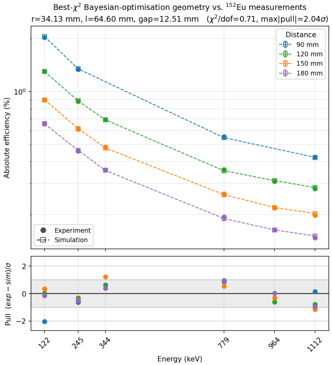

Figure 7: Best-χ^2 geometry vs. ^{152}Eu efficiency measurements, with the pull residual. One point (90 mm/122 keV) reaches 2σ.

- Efficiency depends on the detector's *effective* geometry (dead layer, crystal dimensions, air gap). Murphy et al. 2019: datasheet values can differ from the true response by up to 30%
- **Problem**: brute-force grid search requires 7161 geometries (31 radii $\times$ 7 lengths $\times$ 33 gaps) — impractical to scale
- **Solution**: Bayesian optimisation (fitted to ^{152}Eu efficiency data via a parametric Geant4 model, A. Reina) reduces this to $\sim$100 geometries per distance ($\sim$72$\times$ fewer simulations)
- The campaign converges to within 0.4% of the grid search's best result
- **Cross-validated**: A. Reina's independent grid-based fit agrees to $< 0.6\sigma$ (parameters) and $< 2\%$ (efficiencies, 0.8% avg)

HPGe simulation: calibrating the detector response

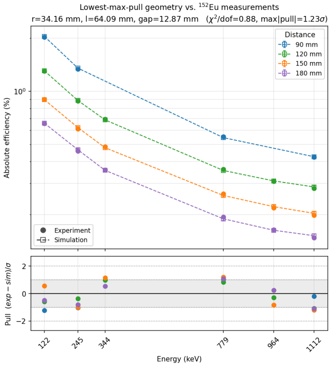

Figure 7: Alternative geometry selected for the smallest worst-case pull: every point within 1.3σ, at a slightly higher χ^2/ndf.

- Efficiency depends on the detector's *effective* geometry (dead layer, crystal dimensions, air gap). Murphy et al. 2019: datasheet values can differ from the true response by up to 30%
- **Problem**: brute-force grid search requires 7161 geometries (31 radii $\times$ 7 lengths $\times$ 33 gaps) — impractical to scale
- **Solution**: Bayesian optimisation (fitted to ^{152}Eu efficiency data via a parametric Geant4 model, A. Reina) reduces this to $\sim$100 geometries per distance ($\sim$72$\times$ fewer simulations)
- The campaign converges to within 0.4% of the grid search's best result
- **Cross-validated**: A. Reina's independent grid-based fit agrees to $< 0.6\sigma$ (parameters) and $<$ 2% (efficiencies, 0.8% avg)

Simulations of the flux at NEAR

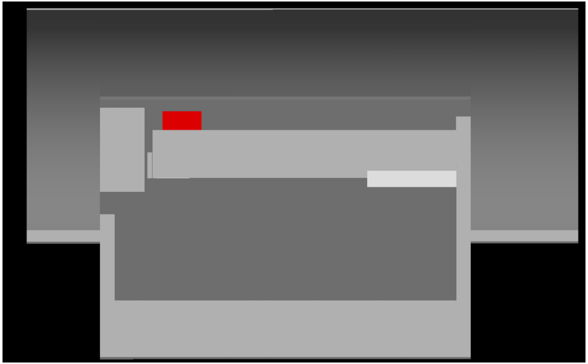

Figure 8: Full Geant4 geometry model of NEAR.

- **Benchmark** vs. absolute SACS
  - Status: validated without the B_4C filter

Simulations of the flux at NEAR

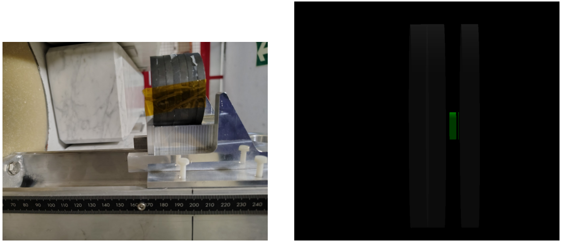

Figure 8: Irradiation setup at NEAR with B4C filters (left) and its Geant4 geometry model (right).

- **Benchmark** vs. absolute SACS
  - Status: validated without the B_4C filter
- **Filter shaping**: Effect of B_4C neutron filters (SACS $\rightarrow$ MACS)
  - Status: ongoing effort combining MCNP/FLUKA/Geant4

Simulations of the flux at NEAR

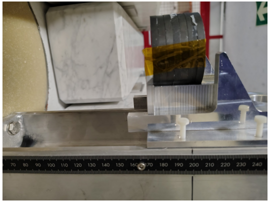

Figure 8: Irradiation setup at NEAR with B4C filters (left) and its Geant4 geometry model (right).

- **Benchmark** vs. absolute SACS
  - Status: validated without the B_4C filter
- **Filter shaping**: Effect of B_4C neutron filters (SACS $\rightarrow$ MACS)
  - Status: ongoing effort combining MCNP/FLUKA/Geant4

Simulations of the flux at NEAR

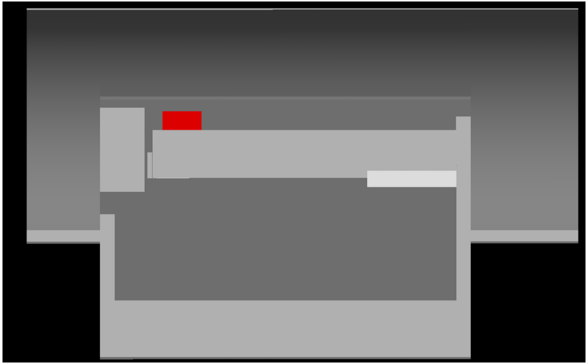

Figure 8: Full Geant4 geometry model of NEAR.

- **Benchmark** vs. absolute SACS
  - Status: validated without the B_4C filter
- **Filter shaping**: Effect of B_4C neutron filters (SACS $\rightarrow$ MACS)
  - Status: ongoing effort combining MCNP/FLUKA/Geant4
- **Room scattering**: scattered-neutron contribution to activation
  - Status: simulations developed in Geant4

Simulations of the flux at NEAR

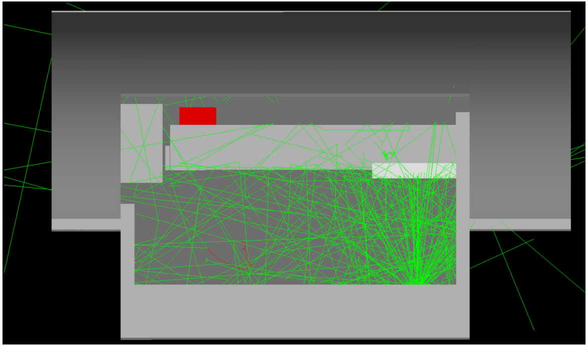

Figure 8: Full Geant4 geometry model of NEAR.

- **Benchmark** vs. absolute SACS
  - Status: validated without the B_4C filter
- **Filter shaping**: Effect of B_4C neutron filters (SACS $\rightarrow$ MACS)
  - Status: ongoing effort combining MCNP/FLUKA/Geant4
- **Room scattering**: scattered-neutron contribution to activation
  - Status: simulations developed in Geant4

1. Motivation & Project Summary
2. Activation experiment at n_TOF-NEAR
3. Progress and results
4. **Conclusion**

Summary

- **Motivation:**
  - Nuclear Astrophysics: s-process discrepancies
  - Nuclear Data: URR discrepancies
  - Facility characterisation: NEAR validation
- **Activation campaign:**
  - NEAR@n_TOF: 3 activations, varying B_4C filtering (incl. one unfiltered), campaign completed
- **Outlook:**
  - Most complete dataset for ^{146}Nd(n,γ)
  - First TOF neutron capture data
  - MACS data at different stellar temperatures
  - Validation and showcase of the NEAR facility
  - New value for the half-life of ^{147}Nd

Thank you!

- bgameiro@ific.uv.es

- PID2022 PhD Contract
- This project has received funding from the European Union's Horizon Europe research and innovation programme under grant agreement No 101057511.

Thank you!

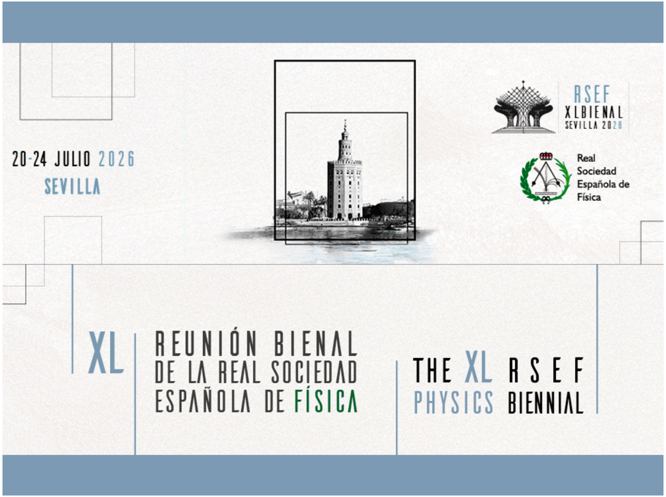
20-24 JULIO 2026
SEVILLA
RSEF
XL BIENAL
SEVILLA 2026
Real
Sociedad
Española de
Física
XL
REUNIÓN BIENAL
DE LA REAL SOCIEDAD
ESPAÑOLA DE FÍSICA
THE XL RSEF
PHYSICS BIENNIAL